DYNAMICS OF COLLISIONAL IONIZATION ASSISTED BY JUDICIOUSLY CHOSEN (BUT NOT VERY STRONG) LASER FIELDS

J. Weiner

JOURNAL DE PHYSIQUE
Colloque C1, supplément au n°1, Tome 46, janvier 1985

DYNAMICS OF COLLISIONAL IONIZATION ASSISTED BY JUDICIOUSLY CHOSEN (BUT NOT VERY STRONG) LASER FIELDS

J. Weiner

University of Maryland, Department of Chemistry, College Park, Maryland 20742, U.S.A.

Résumé - Ce papier présente l'évolution des expériences entreprises dans le domaine de l'ionisation collisionnelle pour mettre en évidence et étudier l'influence d'un champ de radiation modérément intense sur les processus de collisions entre atomes excités.

Abstract- This review traces the evolution of experiments in collisional ionization designed to illustrate and explore the influence of moderately intense optical radiation on the outcome of atomic collisions.

I - EARLY WORK

My research group and I became interested in laser-stimulated events with the observation of Li_2^+ and Li^+ produced by crossed-beam collisions in the presence of a pulsed laser field tuned to the atomic Li resonance line. The essential elements of the experimental layout are illustrated in figure 1. Two effusive atomic beams cross at 90° in the center of an evacuated chamber. Counterpropagating laser beams traverse the interaction center in the same plane as the atomic beams at angles of 45° and 135° with respect to the reference atomic beam axis. Ions produced by collisional processes are accelerated vertically upward by a pulsed electric field and mass analyzed by time-of-flight (TOF) mass spectroscopy. Photon emission can also be detected by an optical system mounted in the same plane as the laser and atomic-beams. Data is accumulated by either boxcar averaging or by waveform digitization.

Figure 2 shows the relative energy levels of the Li_2 and Li_2^+ groundstates. The first experiment employed only a single laser. When tuned to the atomic resonance line, collisions between excited Li*(2p) partners require a minimum additional energy of about 0.41eV to produce Li_2^+ by associative ionization (A.I.). Absorption of a third photon from the laser beam provides 1.85eV, sufficient not only for A.I. but also for Penning ionization (P.I.)

$$Li^*(2p) + Li^*(2p) + \hbar\omega \longrightarrow \begin{cases} Li^+ + Li + e; & \text{(P.I)} \\ Li_2^+ + e; & \text{(A.I.)} \end{cases}$$

Ion intensity therefore should be strongly peaked at the atomic resonance line, Li_2^+ and Li^+ should both be present, and the signal should be linear with laser intensity in the regime where the atomic optical transition is saturated. The results, shown in figures 3 and 4, accord with our expectations. To further test these ideas we added a second laser, counterpropagating as shown in figure 1, and tuned several hundred wavenumbers off-resonance from the atomic transition. Since the third photon needs

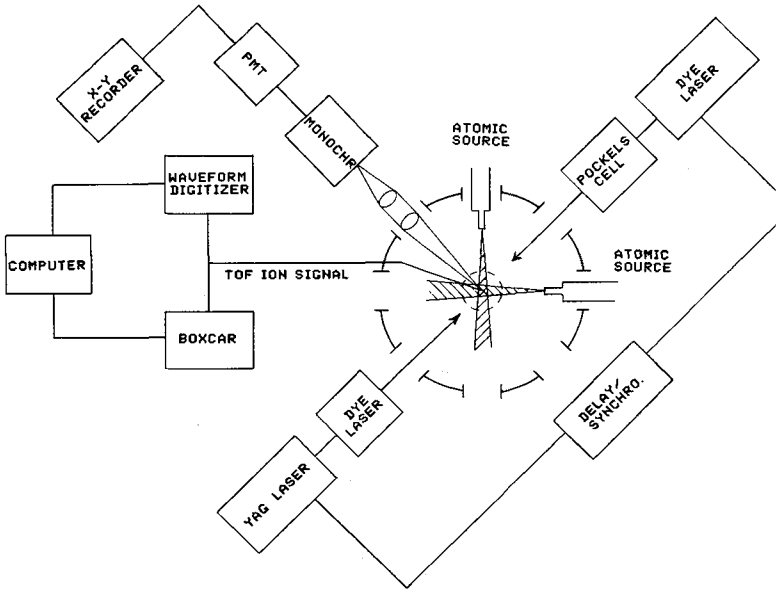

Figure 1: Schematic outline of apparatus.

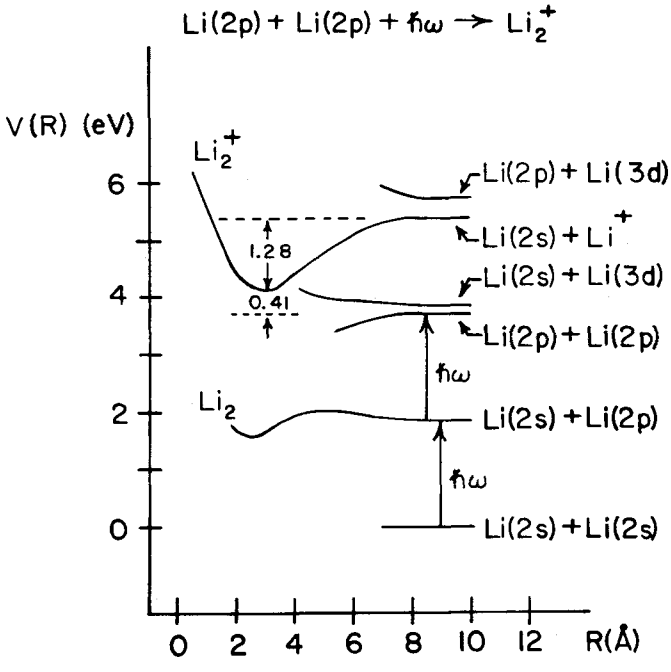

Figure 2: Relevant energy levels of Li_2 and Li_2^+

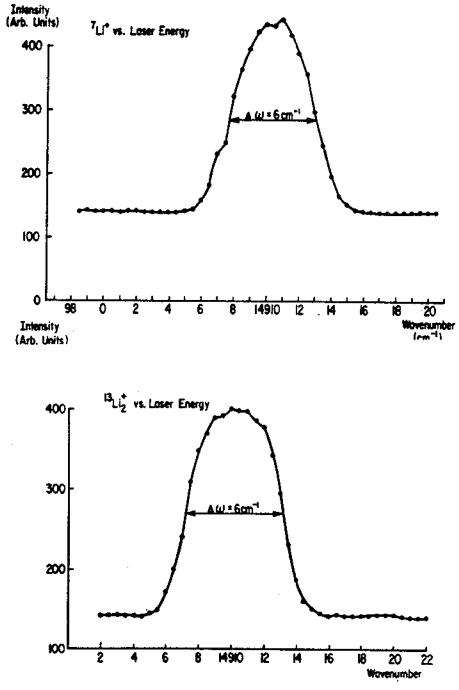

Figure 3: Li^+ and Li_2^+ production vs. laser wavelength. Note peak at Li atomic resonance line.

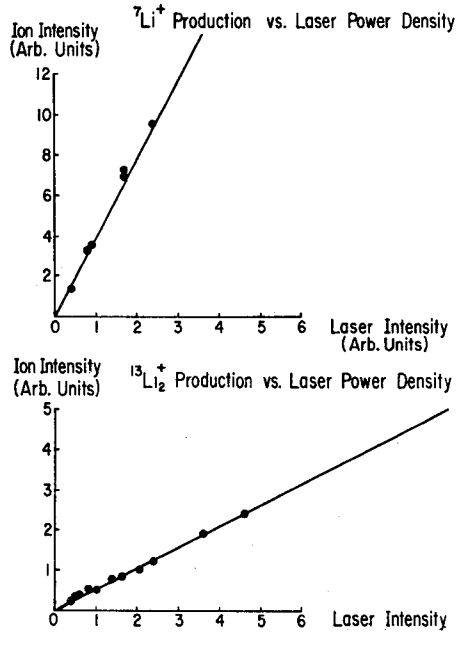

Figure 4: Linearity of signals from laser-induced Penning and associative ionization.

not to be resonant to provide sufficient energy for A.I. and P.I., one might expect enhancement of ion signals from nonresonant photon absorption but only when the first laser is resonantly tuned. Figure 5 demonstrates clearly that nonresonant enhancement indeed takes place as expected when (and only when) the first laser has populated the first excited Li level. These initial experiments tell us little about the nature of laser-induced collision dynamics. They serve only to demonstrate that it exists!

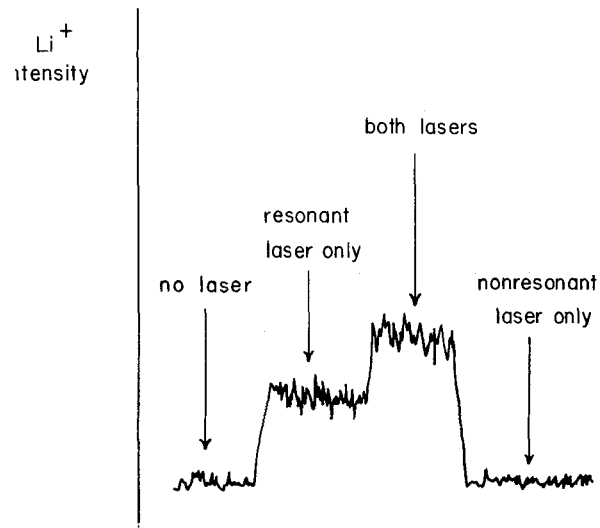

Figure 5: Augmentation of laser-induced signal when a second, nonresonant laser field is added to first laser resonant with Li atomic transition.

We chose next to study collisions between two dissimilar alkali atoms in a second experiment to see if the effect observed in Li-Li was somehow unique to homonuclear species. One might expect so since the long-range electric dipole-dipole interaction gives rise to potential energy splittings varying as the inverse cube of the internuclear separation for homonuclear collisions, while the same interaction in heteronuclear collisions produces potential shifts varying as the inverse sixth power of the internuclear distance. Since the dipole-dipole effect is less pronounced in heteronuclear species, the overall laser-induced collision phenomenon might be more difficult to observe. Figure 6 shows the relevant energy levels in Na-Li system. When the laser is tuned to the Na(3s-3p) transition figure 7 shows that $NaLi^+$ production takes place[2] and figure 8 shows that the ion intensity is linear in laser power. Thus laser-induced A.I. can be demonstrated for heteronuclear collision systems and is not restricted to the homonuclear situation. But having performed these simple observational experiments "pour mettre l'effet en évidence" it is necessary to examine more closely the nature of the collision dynamics.

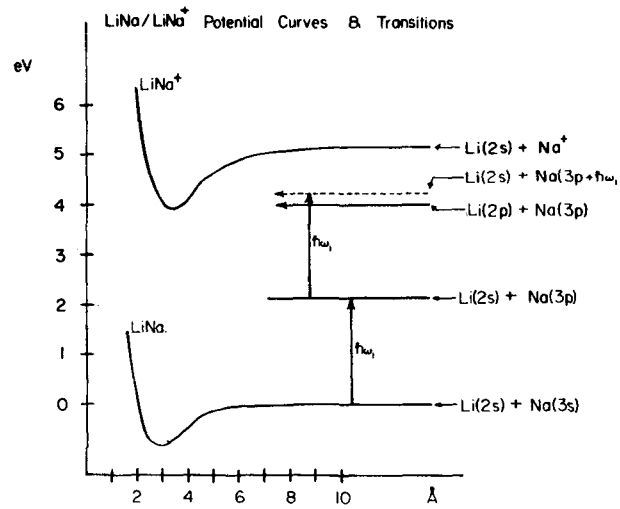

Figure 6: Relevant energy levels and transitions in NaLi and $NaLi^+$.

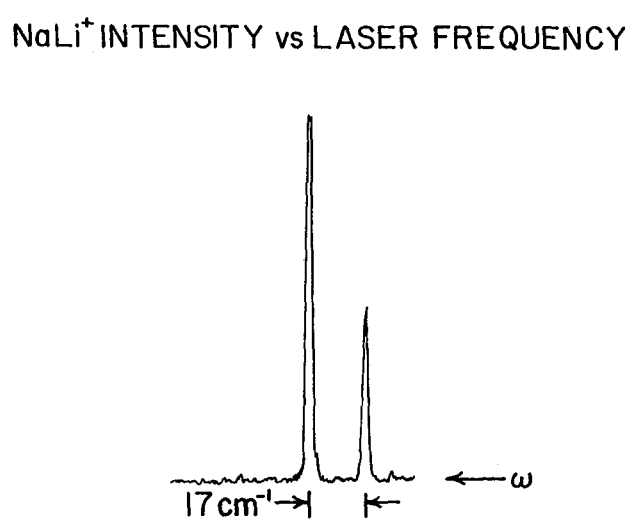

Figure 7: $NaLi^+$ signal vs. laser frequency. Note that peaks appear at Na atomic resonance positions in accord with interpretation of figure 6.

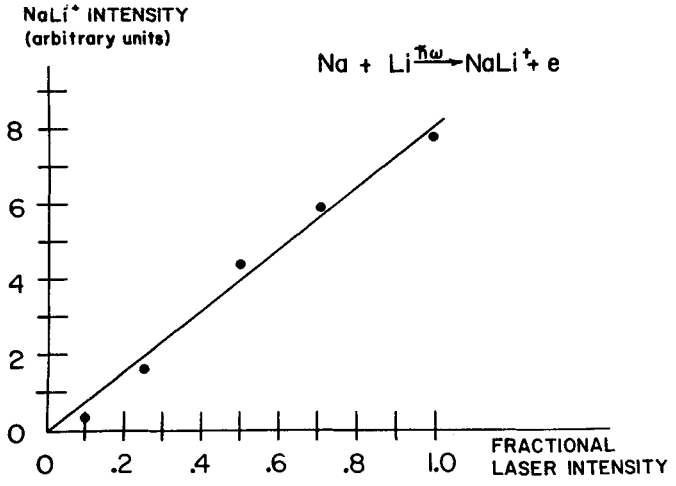

Figure 8: Linearity of $NaLi^+$ vs. laser power density.

II - ALKALI-ALKALINE EARTH EXPERIMENTS

The next set of experiments,[3,4] was designed to investigate the role of long-range forces in laser-induced phenomena. Two complementary experiments were performed:

$$Ba + Na^*(3p) + 2\hbar\omega \longrightarrow Ba^+ + Na(3s) + e \qquad (1)$$

$$Ba^*(6s6p) + Na + 2\hbar\omega \longrightarrow Ba + Na^+ + e \qquad (2)$$

Figure 9 shows the energy level and coupling scheme for process (1). In essence the sequence of events is as follows. An initial laser pulse populates the $Na(3p\ ^2P_{3/2})$ level. This resonantly excited atom approaches a ground state Ba and perturbs it through a long-range van der Waals interaction. The collisional perturbation can be thought of as producing a virtual state in the Ba atom with the energy of the Na(3p) level. Now a second laser pulse ($h\omega_2$) completes the Ba transition from the virtual state to the final excited stationary level $Ba^*\ (6p^2\ ^1S_0)$. This excited level is immediately photoionized in the field of the second laser pulse which yields the final ion product. Note that $h\omega_2$ should be very close to the difference between $Ba(6p^2\ ^1S_0)$ and $Na(3p\ ^2P_{3/2})$ energy levels and that the overall Ba transition is from the ground state $Ba(6s^2\ ^1S_0)$ to $Ba(6p^2\ ^1S_0)$ -- a forbidden transition inaccessible by conventional single photon absorption. The experimental result is shown in figure 10. The peak in the cross section indeed falls close to the expected wavelength. If the van der Waals interaction between two colliding species is dominant, however, a distinct asymmetry in the line shape should extend about 10-20 Å to the long wavlength side of the peak. Although a slight asymmetry can be discerned, it drops off much more sharply than predicted by simple theory.[5] Figure 11 shows that the photon stoichiometry is quadratic because the two-step process requires one photon for the energy transfer and one photon for the photoionization.

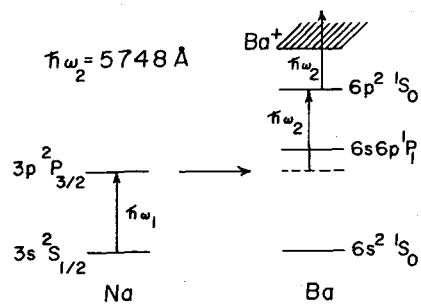

Figure 9: Energy levels of weakly interacting atomic collision between $Na^*(3p)$ and Ba. Note that peak in Ba^+ production occurs at the energy difference between $Ba^*(6p^2\ {}^1S_0)$ and $Na^*({}^2P_{3/2})$.

The roles played by the two colliding species can be reversed. If the Ba ($6s6p\ {}^1P_1$) level is populated by the first laser and the second laser transfers the energy to $Na^*(4d)$ with subsequent photoionization, the process would appear as depicted in figure 12. Here we have shown the quasimolecular curves near their asymptotic limits -- a picture equivalent to that of figure 9. The result is shown in figure 13. As expected a peak appears near the $Na^*(4d)$-Ba($6s6p\ {}^1P_1$) difference energy but again the line shape is narrower than expected. The failure of simple theory to account for the line shape means that the collisional coupling mechanism cannot be described simply by a van der Waals interaction. These results indicate that although the photon interaction is well-understood, the collisional effects are not.

III - OFFRESONANT Na_2^+ PRODUCTION IN SODIUM VAPOR

In an early experiment[6] we reported extensive structure in Na_2^+ production under crossed beam conditions in the presence of two laser fields -- one tuned to the Na resonance line and the other scanned over the range from about 6100 Å to 5750 Å. Figure 14 shows this rich structure in a more recent version of the experiment[7] -- this time with only one laser scanning over the red-orange-yellow-green range of the spectrum. The labeled stick spectrum above the data indicate positions of strong transitions in Doppler-free, two-photon absorption experiments carried out recently by Schawlow[8], et al. The question is: Does the Na_2^+ structure come from multiphoton ionization (MPI) of the small amount of Na_2 in the atomic sodium beams or is it due laser-induced associative ionization between sodium atoms? In order to answer this question we embarked on a two-pronged study. First we performed a series of experiments[7] to test the sensitivity of the Na_2^+ signal to the atomic or dimer population in the reactant beams. Secondly, we undertook to analyze the MPI mechanism[9] in Na_2 dimer so as to determine whether or not it alone could explain the Na_2^+ spectrum.

We tested the atomic origin of Na_2^+ by selectively removing Na population (by atomic photionization) and observing the effect on

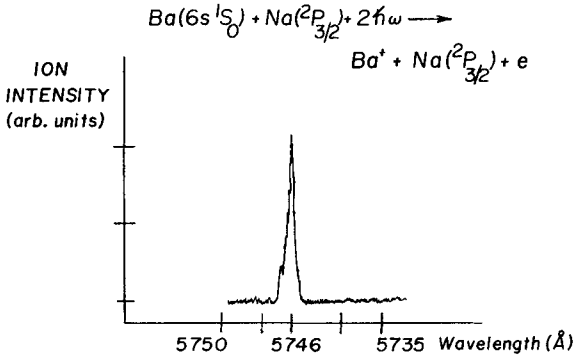

Figure 10: Experimental result of laser-induced, two-photon Penning ionization in Na -Ba collisions (collisional process (1) in text).

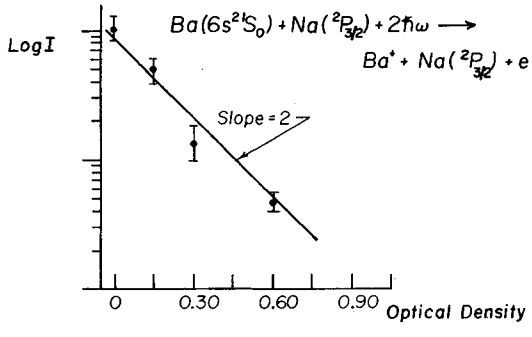

Figure 11: Photon stoichiometery confirming that process (1) requires two photons.

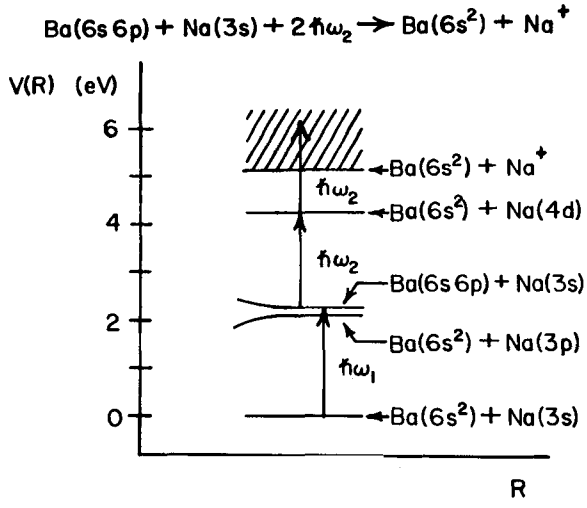

Figure 12: Quasimolecular energy levels relevant to process (2).

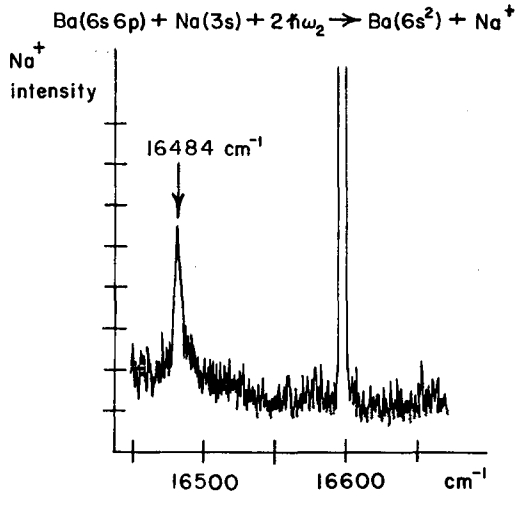

Figure 13: Experimental result showing Na^+ peak at laser frequency corresponding to energy difference between $Na^*(4d)$ and $Ba^*(6s\ 6p\ {}^1P_1)$.

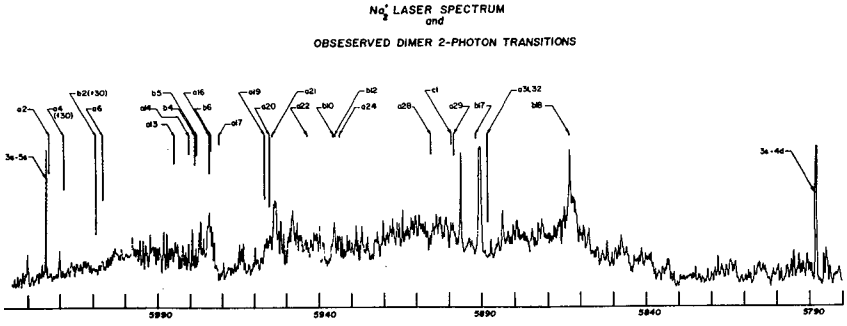

Figure 14: Na_2^+ spectrum vs. laser wavelength. Peak pulse power density ≈ 10^6 W cm^{-2}.

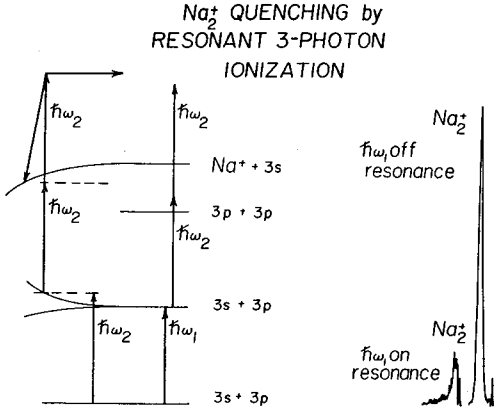

Figure 15: Experiment testing sensitivity of off-resonant Na_2^+ signal to Na atomic population.

the Na_2^+ intensity. Figure 15 summarizes the experiment and the result. The left side of the figure shows two pathways for photon absorption. The far left is a suggested route to Na_2^+ and Na^+ taking place during the course of an atomic collision. Laser 2 ($\hbar\omega_2$) is tuned into the blue wing of the Na resonance line. Long-range resonant dipole forces produce a potential curve splitting which brings the photon into a brief transient resonance with the time-dependant difference potential. A second photon is immediately absorbed into the dense manifold of states associated with the Na(3p), Na(4d), and Na(5s) levels. From this point the system has enough energy to undergo associative ionization, but we have depicted it absorbing yet a third photon to suggest the possibility of an open Penning ionization channel as well. In the experiment we tune $\hbar\omega_2$ to some arbitary position in the red or blue wing and monitor Na_2^+ intensity. This signal is indicated on the far right of the figure. Now the pathway center-left in figure 15 shows what happens if laser 1 ($\hbar\omega_1$) is turned onto the Na(3p) resonance line. Laser 1 saturates the transition; removing about two-thirds of the atomic population from the ground state to the excited level. In the presence of the intense field of laser 2 this population is photoionized by a two-photon process. In effect the action of the two lasers optically pumps the entire atomic population from the ground state into the ionization continuum. The result on the Na_2^+ intensity of this atomic depopulation is shown on the right hand side. The dramatic diminution of the peak labeled "$\hbar\omega_1$ on resonance" occurs <u>only</u> when laser 1 is tuned to the atomic resonance line. We interpret this observation to mean that the atomic MPI process effectively "short-circuits" the laser-induced A.I. pathway by providing a more rapid channel to ionization. Note that the Na_2^+ signal does not disappear entirely which indeed may indicate a residual contribution due to molecular MPI. In order to investigate this possibility more closely we performed experiments on a dimer beam internally cooled by free-jet expansion.

Figure 16 is a schematic of the apparatus which is essentially an adaptation of the set-up used in the crossed-beam work. Here we have only one supersonic beam. The probe laser is either scanning through the visible range to generate an MPI spectrum or is at fixed UV wavelength with sufficient energy to photoionize directly both the atom and dimer species. The UV beam monitors the relative Na - Na_2 population in the free-jet expansion. On good days the source is capable of producing a beam with approximately 50% dimer concentration. The cooled dimer MPI spectrum is shown in the bottom half of figure 17. Note the striking simplification over the structure exhaibited in figure 14. Internal cooling of the vibrational states to the lowest level and rotational cooling to about 60°K (verified by laser-induced fluorescence) are responsible for clearing up the spectrum. The top half of figure 17 is a calculated spectrum based on a model of MPI illustrated in figure 18. The agreement, although not perfect, is sufficient to show that the model is essentially

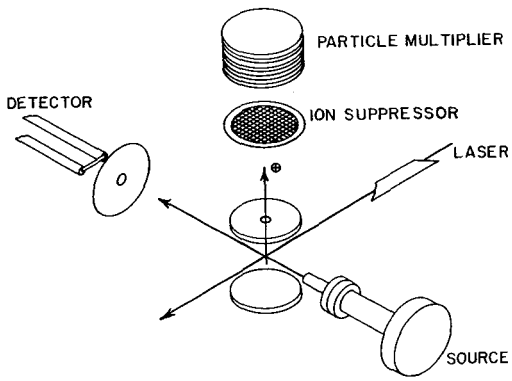

Figure 16: Schematic of apparatus used to study MPI of jet-cooled dimer. Source produces free-jet expansion rather than effusive beam.

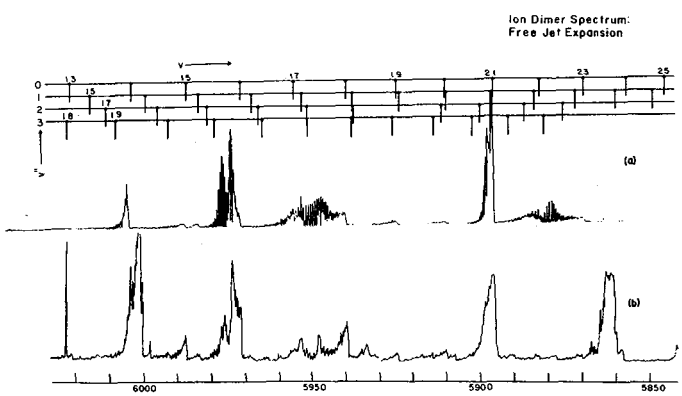

Figure 17: Top spectrum: model calculation; bottom spectrum: measured MPI in jet.

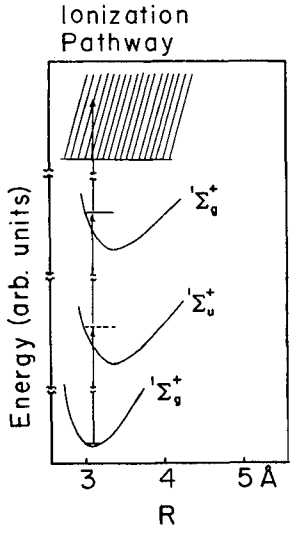

Figure 18: Pathway through excited states of Na_2, producing three-photon (resonantly enchanced) ionization. Note that Na_2 $A(^1\Sigma_u)$ supplies the virtual state coupling between the $X\,^1\Sigma_g$ and $^1\Sigma_g{}^+$ 4d states.

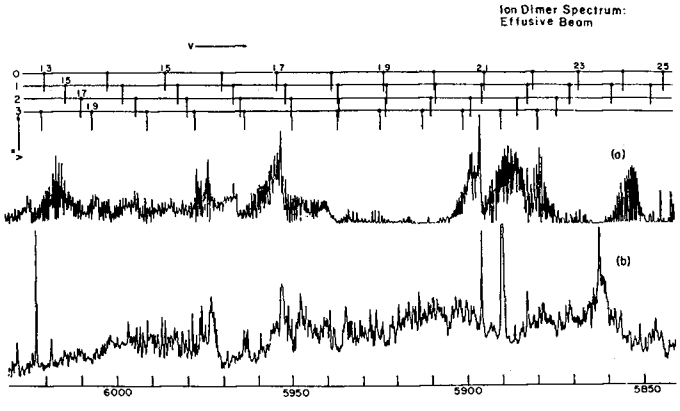

Figure 19: Top spectrum: model calculation; bottom spectrum: measured MPI in effusive beam.

correct[9]. Figure 19 compares the off-resonant spectrum of figure 14 to the same MPI model but with the vibrational-rotational temperatures raised to those typical of an effusive beam. Agreement in the region between 6000Å and 5950Å is not too bad, but elsewhere the model fails to account for many observed structural features. We conclude then that at least some of the Na_2^+ structure is due to dimer MPI but not all of it. Further experiments need to be performed under conditions of negligible dimer concentration so as to completely remove the influence of dimers from the signal.

IV - ASSOCIATIVE IONIZATION DYANMICS BY TOF PHOTOFRAGMENTATION SPECTROSCOPY

Another facet in the overall problem of laser-induced dynamics is the distribution of internal states of the product molecule ions. We have studied the internal state distribution of two A.I. processes,

$$Na^*(6p) + Na(3s) \longrightarrow Na_2^+ + e \qquad (3)$$

$$Na^*(3p) + Na^*(3p) \longrightarrow Na_2^+ + e \qquad (4)$$

by measuring the distribution of recoil energy in the Na^+ fragments when the Na_2^+ formed in (3,4) is photodissociated by monochromatic light

$$Na_2^+ + \hbar\omega \longrightarrow Na^+ + Na \qquad (5)$$

Figure 20 shows the relevant energy level diagram. In the case of (3) we see that vibrational levels from about v = 40 are energetically accessible. For fixed $h\nu$ (from the photodissociation laser) the actual distribution of vibrational population will be reflected in the photofragment recoil energy, W. The experimental set-up is shown in figure 21. First a laser tuned to an atomic transition prepares the colliding partners in states suitable for A.I. to take place. The collisional interaction region is then sampled by a pulsed electric field that draws the ions vertically into a second, drift region where the ion packet is photodissociated. The TOF spectrum of both the fragments and the parent are finally detected at the end of the drift region. Figure 22 shows a typical parent-peak spectrum, indicating the narrow time dispersion in the Na_2^+ ion packet. Figures 23 and 24 show the results for processes (3,4). In both cases the recoil energy peaks at the maximum in the Maxwell-Boltzmann distribution of relative collision energies and the W distribution is smooth with apparently all energetically available vibrational energy levels filled. In particular figure 24 shows no evidence of a previously suggested bimodel internal energy distribution in process (4).

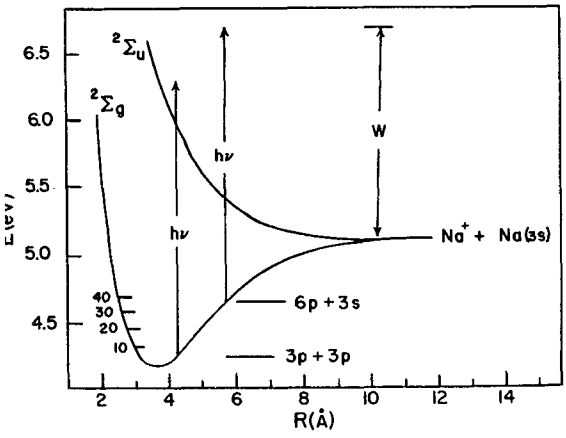

Figure 20: Molecular curves relevant to photofragmentation of Na_2^+ formed by associative ionization. The quantity W is the recoil energy from which the internal state distribution of parent Na_2^+ can be inferred.

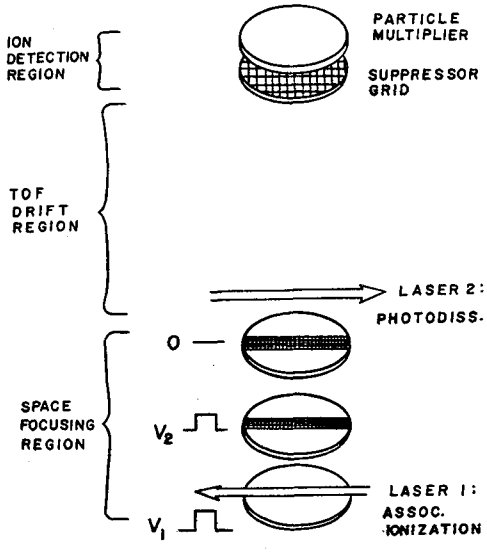

Figure 21: Schematic of Na_2^+ photofragmentation experiment.

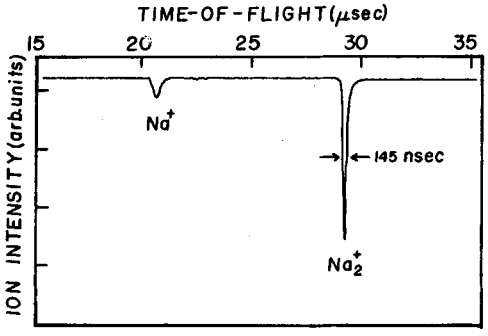

Figure 22: Parent peaks in Na_2^+ photofragmentation experiment. Note narrow time dispersion of Na_2^+ ion packet.

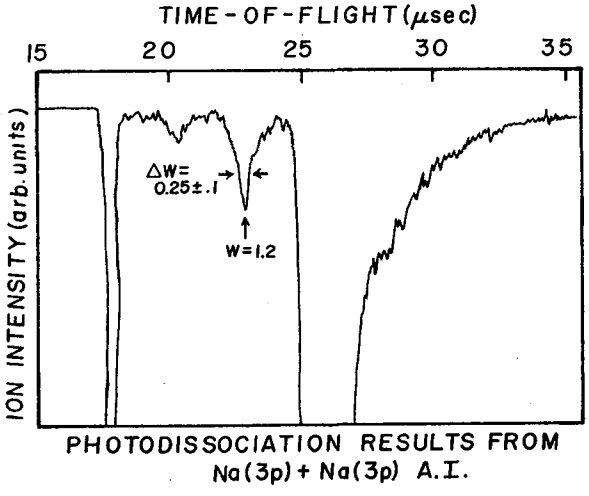

Figure 23: Recoil velocity distribution of Na^+ fragment from process (3).

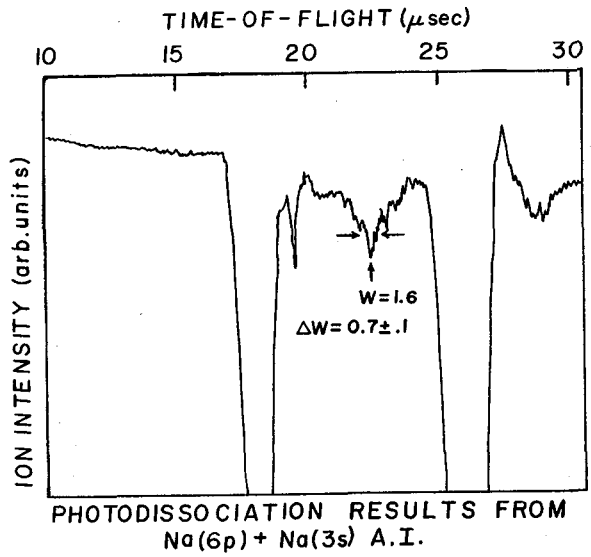

Figure 24: Recoil velocity distribution of Na^+ fragment from process (4).

V - HALF-COLLISION SPECTROSCOPY AND DYNAMICS -- DETERMINATION OF THE ELECTRONIC BARRIER HEIGHT IN Na_2 ($B^1\Pi_u$)

The final topic in this report concerns the use of free-jet expansions and high-resolution lasers to reveal subtle aspects of both the structure and dynamics of collisional quasimolecules. The specific problem is determination of the barrier height in Na_2 ($B^1\Pi_u$), but the techniques applied to its solution point the way to a fruitful line of research on the dissociation dynamics of excited molecules. Interactions such as spin-orbit, hyperfine, or Coriolis coupling between adiabatic states can profoundly influence the final states of the dissociated partners. By measuring these final states we can begin to understand half-collision processes which undoubtedly play an important role in laser-induced processes as well.

To begin with we employ an optical pumping scheme (steps 6 and 7 below) to prepare Na_2 in vibrational states favorable to dissociation:

$$Na_2\ (X^1\Sigma_g) + \hbar\omega_1 \longrightarrow Na_2^*\ (A^1\Sigma_u);\ v' = 0\text{-}4 \qquad (6)$$

$$Na_2^*\ (A\ ^1\Sigma_u) \rightsquigarrow Na_2^\dagger\ (X\ ^1\Sigma_g);\ v'' = 9,10,11 \text{ etc} \qquad (7)$$

$$Na_2^\dagger + \hbar\omega_2 \longrightarrow Na^*\ (3p) + Na\ (^2S_{1/2}) \qquad (8)$$

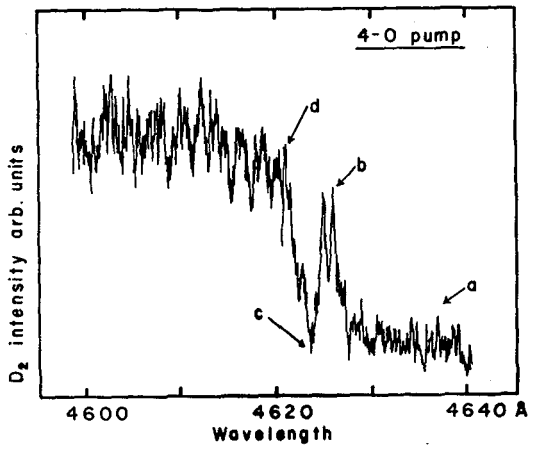

Figure 25: Threshold for photodissociation of Na_2 from B ($^1\Pi_u$) state. Note quasibound vibrational level just before the onset.

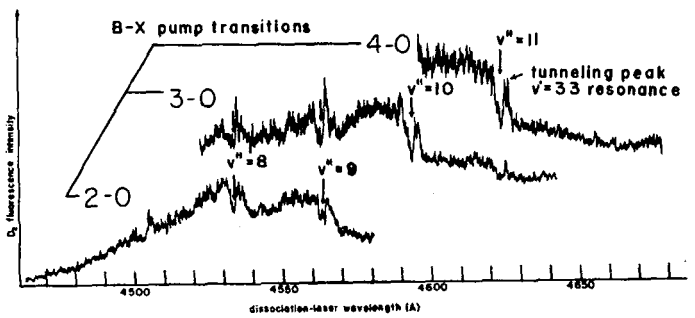

Figure 26: Confirmation of result shown in figure 25 from several different pump transitions.

Step (8) is the final dissociation to one excited and one ground state atom. We expect a sharp onset of Na^* (3p) fluorescence as laser 2 ($h\omega_2$) is scanned through the barrier height. Relative intensity of D_1 to D_2 emission will yield immediately information on nonadiabatic coupling since a purely adiabatic dissociation would result only in population of the Na (3p $^2P_{3/2}$) level. Figure 25 shows the sharp onset of D_2 emission between (c) and (d) as expected. The feature at (b) is the last quasibound vibrational state of Na_2 (B $^1\Pi_u$). Its position and width allow us to infer the shape of the barrier near its maximum. Figure 26 shows that by using several pump transitions we can scan laser 2 over the barrier height at several different spectral positions depending on the vibrational level pumped by laser 1. The value of the barrier height turns out to be 367 cm^{-1} ± 8 cm^{-1} and the observation of only D_2 emission indicates an essentially adiabatic dissociation. The interest in this experiment, however, is in its potential more than in its result. By using a laser with a resolution of about 20 MHz, individual rotational states can be prepared before dissociation. Probing individual M_J sublevels of Na (3p $^2P_{3/2}$) after dissociation as a function of rotational energy before dissociation will lead to a direct determination of the importance of Coriolis coupling in nonadiabatic dissocation dynamics. We believe that experiments along this line promise to yield a clearer understanding of coupling processes which in turn will inform our experiments on laser-induced collisional ionization.

REFERENCES

1. A.v. Hellfeld, J. Caddick, and J. Weiner, Phys. Rev. Lett. 40, (1978) 1369.
2. P. Polak-Dingels, J.-C. Gauthier, J. Keller, M. Bras, and J. Weiner, Phys. Rev. A 24, (1981) 1107.
3. J. Keller and J. Weiner, Phys. Rev. A 29, (1984) 2230.
4. P. Polak-Dingels, J. Keller, R. Bonanno, and J. Weiner, J. Phys. B: At. Mol. Phys 15 (1982) L41-L44.
5. S.E. Harris and J.C. White, IEEE J. Quant. Elec. QE-13 (1977) 972.
6. P. Polak-Dingels, J.-F. Delpech, and J. Weiner, Phys. Rev. Lett. 44 (1980) 1663.
7. Jacques Boulmer and J. Weiner, Phys. Rev. A 27 (1983) 2817.
8. C.P. Morgan, H.R. Xia, and A.L. Schawlow, J. Opt. Soc. Am. 72, (1982) 315.
9. J. Keller and J. Weiner, Phys. Rev. A. (1984) (in press).
10. J. Keller and J. Weiner, Phys. Rev. A. 29 (1984) (in press).